Low-temperature ordered states of rare-earth magnetic dipoles in $R_2Ba_4Cu_7O_{15-\delta}$ as effected by dipole-dipole and exchange interactions: Extension of generalized Luttinger-Tisza method

Sushil K. Misra[1] and Joshua Felsteiner[2]
[1]*Physics Department, Concordia University, 1455 de Maisonneuve Boulevard West, Montreal, Quebec, Canada H3G 1M8*
[2]*Physics Department, Technion-Israel Institute of Technology, 32000 Haifa, Israel*
(Received 30 August 2002; revised manuscript received 19 November 2002; published 7 April 2003)

The lowest energies and the corresponding low-temperature orderings of the magnetic moments in the high-T_c superconducting compounds $R_2Ba_4Cu_7O_{15-\delta}$ (R=rare earth) have been calculated by extending the Luttinger-Tisza technique to include 32 sublattices of the magnetic R^{3+} ions, taking into account dipolar and exchange interactions. The calculated lowest energy configurations for Dy247 and Er247 compounds, the only ones investigated experimentally as to magnetic orderings, are found to be consistent with those determined by neutron-scattering experiments.

DOI: 10.1103/PhysRevB.67.144505 PACS number(s): 75.25.+z

I. INTRODUCTION

The high-temperature superconducting compound (HTSC) $Yb_2Ba_4Cu_7O_{15-\delta}$ (hereafter Yb247) was produced in 1988 by oxidizing metallic precursors in 1-bar O_2 by Kogure *et al.*,[1] consisting of alternating blocks of $YbBa_2Cu_4O_8$ (hereafter Yb124) and $YbBa_2Cu_3O_{7-\delta}$ (hereafter Yb123) along the *c* axis. Subsequently, isolated crystals of Y247 were found by Bordet *et al.*[2] in a melt of Y123, subjected to 100-bar oxygen pressure. Later, preparation of the HTSC Y247 in bulk, as well as five analogous rare-earth compounds *R*247 (*R*=rare-earth) with *R*=Eu, Gd, Dy, Ho, and Er, was reported by Morris *et al.*[3] using the solid-state reaction method, with moderate oxygen pressures ranging from 11–35 bars. The superconducting transition temperature T_c of Y247 (T_c=55 K) is much lower than those of Y123 (T_c=92 K) and Y124 (T_c=81 K). Thus a detailed comparison of the properties of the *R*247 compounds with the *R*123 and *R*124 compounds may help unravel the mechanism underlying the superconductivity of the HTSC compounds. More details of these comparisons relating to T_c and diamagnetism, x-ray diffraction, phase diagrams, variable-oxygen stoichiometry, correlation of structural parameters with T_c, and variation of lattice parameters and T_c with rare-earth substitution, were reported by Morris *et al.*[3] Further investigations by Tallon *et al.*[4] of superconductivity in *R*247 compounds as a function of oxygen stoichiometry found T_c to decrease monotonically with δ, from a maximum of 92 K when δ=0 to a minimum of 30 K when δ=1.0. In addition, the compounds were found to remain orthorhombic for all values of δ. The lattice parameters for several *R*247 compounds as reported by Morris *et al.*,[3] by Zhang *et al.*,[5] and by Böttger *et al.*[6] are listed in Table I.

As for experimental investigations, the magnetic properties of Er247 and Dy247 compounds were studied by Böttger *et al.*[7] by specific-heat measurements. They reported that a magnetic phase transition occurred in Er247 at T_N=0.54 K for $\delta\sim$0.1 and at T_N=0.50 K for $\delta\sim$0.7, and concluded, in conjunction with inelastic neutron-scattering data, that while the specific-heat data with δ=0.08 can be interpreted with an isotropic two-dimensional (2D) Ising model, the corresponding data of Er247 with δ=0.7 can only be understood by assuming two different types of magnetic clusters to be present in this compound. They emphasized the importance of dipolar and superexchange interactions for the observed magnetic ordering. The neutron-diffraction experiments of Böttger *et al.*[6] revealed that the coupling of Er^{3+} ions in Er247 with δ=0.1 along the *a* axis is antiferromagnetic ($J<0$), whereas it is ferromagnetic along the *b* axis ($J>0$). Further, Böttger *et al.*[7–9] interpreted their specific-heat data on Er247 by the use of an anisotropic 2D Ising model with the anisotropy $|J_2/J_1|$ being $\frac{1}{4}$, choosing opposite signs for J_1 and J_2 of Er^{3+} ions. The values of J_1, J_2 so estimated, are, respectively, in units of K, +0.452, −0.104 (or −0.452, +0.104) for Er247 and −0.811, −0.197 for Dy247. Zhang *et al.*[5,10] analyzed their neutron-diffraction data on Dy247 in terms of coupled two-dimensional (2D) bilayer magnetic order of Dy ions, wherein the Dy spins within the *a*-*b* planes are coupled antiferromagnetically with T_N=1.25 K. Further, they deduced that the 2D order originated from the crystal structure, as the *c*-axis spacing of the magnetic ions was ~3 times the *a*, *b* spacing. In addition, every other *a*-*b* plane was shifted along the *b* axis by *b*/2, causing a cancellation of magnetic interactions which completely isolated the bilayers. They anticipated occurrence of similar coupled bilayer 2D behavior in other *R*247 compounds in which the nearest-neighbor spins were coupled antiferromagnetically within the *a*-*b* plane. They found similarity of their results on Dy247 to those on Dy123 and Dy124 compounds.

Recently, the expected low-temperature ordered states of rare-earth sublattices for the lowest energy states were cal-

TABLE I. Experimentally determined lattice parameters (Å) for various *R*247 compounds.

Compound	*a*	*b*	*c*	Reference
Gd247	3.872	3.879	50.36	3
Dy247	3.864	3.879	50.39	3
Dy247	3.864	3.879	50.26	5
Er247	3.847	3.873	50.44	3
Er247	3.8263	3.8663	50.3683	6

TABLE II. Permutation groups P_t ($t=1,2,...,32$) of 32 objects. It is easily seen that $[P_t, P_{t'}]=0$ for $t \neq t'$.

$P_1 = I$ (Identity)
$P_2 = (1,2)(3,4)(5,6)(7,8)(9,10)(11,12)(13,14)(15,16)(17,18)(19,20)(21,22)(23,24)(25,26)(27,28)(29,30)(31,32)$
$P_3 = (1,3)(2,4)(5,7)(6,8)(9,11)(10,12)(13,15)(14,16)(17,19)(18,20)(21,23)(22,24)(25,27)(26,28)(29,31)(30,32)$
$P_4 = (1,4)(2,3)(5,8)(6,7)(9,12)(10,11)(13,16)(14,15)(17,20)(18,19)(21,24)(22,23)(25,28)(26,27)(29,32)(30,31)$
$P_5 = (1,5)(2,6)(3,7)(4,8)(9,13)(10,14)(11,15)(12,16)(17,21)(18,22)(19,23)(20,24)(25,29)(26,30)(27,31)(28,32)$
$P_6 = (1,6)(2,5)(3,8)(4,7)(9,14)(10,13)(11,16)(12,15)(17,22)(18,21)(19,24)(20,23)(25,30)(26,29)(27,32)(28,31)$
$P_7 = (1,7)(2,8)(3,5)(4,6)(9,15)(10,16)(11,13)(12,14)(17,23)(18,24)(19,21)(20,22)(25,31)(26,32)(27,29)(28,30)$
$P_8 = (1,8)(2,7)(3,6)(4,5)(9,16)(10,15)(11,14)(12,13)(17,24)(18,23)(19,22)(20,21)(25,32)(26,31)(27,30)(28,29)$
$P_9 = (1,9)(2,10)(3,11)(4,12)(5,13)(6,14)(7,15)(8,16)(17,25)(18,26)(19,27)(20,28)(21,29)(22,30)(23,31)(24,32)$
$P_{10} = (1,10)(2,9)(3,12)(4,11)(5,14)(6,13)(7,16)(8,15)(17,26)(18,25)(19,28)(20,27)(21,30)(22,29)(23,32)(24,31)$
$P_{11} = (1,11)(2,12)(3,9)(4,10)(5,15)(6,16)(7,13)(8,14)(17,27)(18,28)(19,25)(20,26)(21,31)(22,32)(23,29)(24,30)$
$P_{12} = (1,12)(2,11)(3,10)(4,9)(5,16)(6,15)(7,14)(8,13)(17,28)(18,27)(19,26)(20,25)(21,32)(22,31)(23,30)(24,29)$
$P_{13} = (1,13)(2,14)(3,15)(4,16)(5,9)(6,10)(7,11)(8,12)(17,29)(18,30)(19,31)(20,32)(21,25)(22,26)(23,27)(24,28)$
$P_{14} = (1,14)(2,13)(3,16)(4,15)(5,10)(6,9)(7,12)(8,11)(17,30)(18,29)(19,32)(20,31)(21,26)(22,25)(23,28)(24,27)$
$P_{15} = (1,15)(2,16)(3,13)(4,14)(5,11)(6,12)(7,9)(8,10)(17,31)(18,32)(19,29)(20,30)(21,27)(22,28)(23,25)(24,26)$
$P_{16} = (1,16)(2,15)(3,14)(4,13)(5,12)(6,11)(7,10)(8,9)(17,32)(18,31)(19,30)(20,29)(21,28)(22,27)(23,26)(24,25)$
$P_{17} = (1,17)(2,18)(3,19)(4,20)(5,21)(6,22)(7,23)(8,24)(9,25)(10,26)(11,27)(12,28)(13,29)(14,30)(15,31)(16,32)$
$P_{18} = (1,18)(2,17)(3,20)(4,19)(5,22)(6,21)(7,24)(8,23)(9,26)(10,25)(11,28)(12,27)(13,30)(14,29)(15,32)(16,31)$
$P_{19} = (1,19)(2,20)(3,17)(4,18)(5,23)(6,24)(7,21)(8,22)(9,27)(10,28)(11,25)(12,26)(13,31)(14,32)(15,29)(16,30)$
$P_{20} = (1,20)(2,19)(3,18)(4,17)(5,24)(6,23)(7,22)(8,21)(9,28)(10,27)(11,26)(12,25)(13,32)(14,31)(15,30)(16,29)$
$P_{21} = (1,21)(2,22)(3,25)(4,24)(5,17)(6,18)(7,19)(8,20)(9,29)(10,30)(11,31)(12,32)(13,25)(14,26)(15,27)(16,28)$
$P_{22} = (1,22)(2,21)(3,24)(4,25)(5,18)(6,17)(7,20)(8,19)(9,30)(10,29)(11,32)(12,31)(13,26)(14,25)(15,28)(16,27)$
$P_{23} = (1,23)(2,24)(3,21)(4,22)(5,19)(6,20)(7,17)(8,18)(9,31)(10,32)(11,29)(12,30)(13,27)(14,28)(15,25)(16,26)$
$P_{24} = (1,24)(2,23)(3,22)(4,21)(5,20)(6,19)(7,18)(8,17)(9,32)(10,31)(11,30)(12,29)(13,28)(14,27)(15,26)(16,25)$
$P_{25} = (1,25)(2,26)(3,27)(4,28)(5,29)(6,30)(7,31)(8,32)(9,17)(10,18)(11,19)(12,20)(13,21)(14,22)(15,23)(16,24)$
$P_{26} = (1,26)(2,25)(3,28)(4,27)(5,30)(6,29)(7,32)(8,31)(9,18)(10,17)(11,20)(12,19)(13,22)(14,21)(15,24)(16,23)$
$P_{27} = (1,27)(2,28)(3,25)(4,26)(5,31)(6,32)(7,29)(8,30)(9,19)(10,20)(11,17)(12,18)(13,23)(14,24)(15,21)(16,22)$
$P_{28} = (1,28)(2,27)(3,26)(4,25)(5,32)(6,31)(7,30)(8,29)(9,20)(10,19)(11,18)(12,17)(13,24)(14,23)(15,22)(16,21)$
$P_{29} = (1,29)(2,30)(3,31)(4,32)(5,25)(6,26)(7,27)(8,28)(9,21)(10,22)(11,23)(12,24)(13,17)(14,18)(15,19)(16,20)$
$P_{30} = (1,30)(2,29)(3,32)(4,31)(5,26)(6,25)(7,28)(8,27)(9,22)(10,21)(11,24)(12,23)(13,18)(14,17)(15,20)(16,19)$
$P_{31} = (1,31)(2,32)(3,29)(4,30)(5,27)(6,28)(7,25)(8,26)(9,23)(10,24)(11,21)(12,22)(13,19)(14,20)(15,17)(16,18)$
$P_{32} = (1,32)(2,31)(3,30)(4,29)(5,28)(6,27)(7,26)(8,25)(9,24)(10,23)(11,22)(12,21)(13,20)(14,19)(15,18)(16,17)$

culated on the basis of dipolar and exchange interactions among R^{3+} ions using the Luttinger-Tisza (LT) method,[11] as generalized by Misra,[12] in $R123$ compounds by Misra and Felsteiner[13] and by Anders and Volotskii.[14] These calculations were further extended by Felsteiner and Misra[15] to $R124$ compounds. The superconducting $R123$ and $R124$ compounds are both nearly tetragonal with a slight orthorhombic distortion, the unit-cell parameter b being slightly greater than a for both types of compounds. Although, the c/a ratios are different in these two compounds, ~ 3 in $R123$ and ~ 7 in $R124$, it turns out that the c-axis spacing of the rare-earth ions is ~ 3 times the a-b spacing for both the $R123$ and $R124$ compounds, because while there is only one R^{3+} ion per unit cell in $R123$, there are two R^{3+} ions per unit cell in $R124$. Similarly, for $R247$ compounds, although the c/a ratio ~ 13, the c-axis spacing turns out to be ~ 3 times the a-b spacing here also as there exist four ions per unit cell.

It is the purpose of this paper to calculate the lowest energy configurations of the magnetic moments of the rare-earth ions in $R247$ compounds prevalent at low temperatures due to dipole-dipole and exchange interactions amongst the R^{3+} ions. This is accomplished by using the generalized LT method[12] to take into account 32 sublattices required for the presence of four R^{3+} ions per unit cell. The results required to extend the LT method to calculate the lowest energy states of $R247$ compounds are described in Sec. II. The resulting energies and lowest-energy configurations of the R^{3+} ions in the various $R247$ compounds are discussed in Sec. III, while the particular results for Dy247 and Er247 compounds, the only ones investigated experimentally, are described in Sec. IV.

II. RESULTS REQUIRED TO EXTEND THE LUTTINGER-TISZA METHOD USING PERMUTATION GROUPS TO 32 SUBLATTICES

Applications of the general LT method using permutation groups to calculate the lowest energy configurations of $R123$ and $R124$ compounds involving 8 and 16 sublattices were

TABLE III. The normalized eigenvectors $\mathbf{q}(\mathbf{k})$; $k=1,2,3,...,32$ for the operators of permutation groups of 32 objects as listed in Table II.

1	2	3	4	5	6	7	8	9	10	11	12	13	14	15	16	17	18	19	20	21	22	23	24	25	26	27	28	29	30	31	32
α	α	α	α	β	β	β	β	γ	γ	γ	γ	α	α	α	α	δ	δ	δ	δ	γ	γ	γ	γ	β	β	β	β	δ	δ	δ	δ
α	α	α	α	b	b	b	b	γ	γ	γ	γ	a	a	a	a	δ	δ	δ	δ	g	g	g	g	β	β	β	β	d	d	d	d
α	α	a	a	β	β	b	b	γ	γ	g	g	α	α	a	a	δ	δ	d	d	γ	γ	g	g	β	β	b	b	δ	δ	d	d
α	α	a	a	b	b	β	β	γ	γ	g	g	a	a	α	α	δ	δ	d	d	g	g	γ	γ	β	β	b	b	d	d	δ	δ
α	a	α	a	β	b	β	b	γ	g	γ	g	α	a	α	a	δ	d	δ	d	γ	g	γ	g	β	b	β	b	δ	d	δ	d
α	a	α	a	b	β	b	β	γ	g	γ	g	a	α	a	α	δ	d	δ	d	g	γ	g	γ	β	b	β	b	d	δ	d	δ
α	a	a	α	β	b	b	β	γ	g	g	γ	α	a	a	α	δ	d	d	δ	γ	g	g	γ	β	b	b	β	δ	d	d	δ
α	a	a	α	b	β	β	b	γ	g	g	γ	a	α	α	a	δ	d	d	δ	g	γ	γ	g	β	b	b	β	d	δ	δ	d

In the table above, The α, a, β, b, γ, g, δ, d are four-column vectors, whose elements are defined as follows:

$$\sqrt{32}\alpha=-\sqrt{32}a=\begin{pmatrix}1\\1\\1\\1\end{pmatrix};\quad \sqrt{32}\beta=-\sqrt{32}b=\begin{pmatrix}1\\-1\\-1\\1\end{pmatrix};\quad \sqrt{32}\gamma=-\sqrt{32}g=\begin{pmatrix}1\\1\\-1\\-1\end{pmatrix};\quad \sqrt{32}\delta=-\sqrt{32}d=\begin{pmatrix}1\\-1\\1\\-1\end{pmatrix}.$$

TABLE IV. Eigenvalues ε_{kj} corresponding to the eigenvectors $q(k)$ for the operators of permutation groups P_k of 32 objects as given by Eq. (1), and listed in Table II. Here + and − stand for +1 and −1, respectively. In the following table, the row (as counted from left to right) and column (as counted from top to bottom) numbers correspond to the index k and j, respectively.

+	+	+	+	+	+	+	+	+	+	+	+	+	+	+	+	+	+	+	+	+	+	+	+	+	+	+	+	+	+	+	+
+	+	+	+	+	+	+	+	+	+	+	+	+	+	+	+	−	−	−	−	−	−	−	−	−	−	−	−	−	−	−	−
+	+	+	+	+	+	+	+	−	−	−	−	−	−	−	−	+	+	+	+	+	+	+	+	−	−	−	−	−	−	−	−
+	+	+	+	+	+	+	+	−	−	−	−	−	−	−	−	−	−	−	−	−	−	−	−	+	+	+	+	+	+	+	+
+	−	−	+	−	+	+	−	+	−	−	+	−	+	+	−	+	−	−	+	−	+	+	−	+	−	−	+	−	+	+	−
+	−	−	+	−	+	+	−	+	−	−	+	−	+	+	−	−	+	+	−	+	−	−	+	−	+	+	−	+	−	−	+
+	−	−	+	−	+	+	−	−	+	+	−	+	−	−	+	+	−	−	+	−	+	+	−	−	+	+	−	+	−	−	+
+	−	−	+	−	+	+	−	−	+	+	−	+	−	−	+	−	+	+	−	+	−	−	+	+	−	−	+	−	+	+	−
+	+	−	−	+	+	−	−	+	+	−	−	+	+	−	−	+	+	−	−	+	+	−	−	+	+	−	−	+	+	−	−
+	+	−	−	+	+	−	−	+	+	−	−	+	+	−	−	−	−	+	+	−	−	+	+	−	−	+	+	−	−	+	+
+	+	−	−	+	+	−	−	−	−	+	+	−	−	+	+	+	+	−	−	+	+	−	−	−	−	+	+	−	−	+	+
+	+	−	−	+	+	−	−	−	−	+	+	−	−	+	+	−	−	+	+	−	−	+	+	+	+	−	−	+	+	−	−
+	+	+	+	−	−	−	−	+	+	+	+	−	−	−	−	+	+	+	+	−	−	−	−	+	+	+	+	−	−	−	−
+	+	+	+	−	−	−	−	+	+	+	+	−	−	−	−	−	−	−	−	+	+	+	+	−	−	−	−	+	+	+	+
+	+	+	+	−	−	−	−	−	−	−	−	+	+	+	+	+	+	+	+	−	−	−	−	−	−	−	−	+	+	+	+
+	+	+	+	−	−	−	−	−	−	−	−	+	+	+	+	−	−	−	−	+	+	+	+	+	+	+	+	−	−	−	−
+	−	+	−	+	−	+	−	+	−	+	−	+	−	+	−	+	−	+	−	+	−	+	−	+	−	+	−	+	−	+	−
+	−	+	−	+	−	+	−	+	−	+	−	+	−	+	−	−	+	−	+	−	+	−	+	−	+	−	+	−	+	−	+
+	−	+	−	+	−	+	−	−	+	−	+	−	+	−	+	+	−	+	−	+	−	+	−	+	−	−	+	−	+	−	+
+	−	+	−	+	−	+	−	−	+	−	+	−	+	−	+	−	+	−	+	−	+	−	+	+	−	+	−	+	−	+	−
+	+	−	−	−	−	+	+	+	+	−	−	−	−	+	+	+	+	−	−	−	−	+	+	+	+	−	−	−	−	+	+
+	+	−	−	−	−	+	+	+	+	−	−	−	−	+	+	−	−	+	+	+	+	−	−	−	−	+	+	+	+	−	−
+	+	−	−	−	−	+	+	−	−	+	+	+	+	−	−	+	+	−	−	−	−	+	+	−	−	+	+	+	+	−	−
+	+	−	−	−	−	+	+	−	−	+	+	+	+	−	−	−	−	+	+	+	+	−	−	+	+	−	−	−	−	+	+
+	−	−	+	+	−	−	+	+	−	−	+	+	−	−	+	+	−	−	+	+	−	−	+	+	−	−	+	+	−	−	+
+	−	−	+	+	−	−	+	+	−	−	+	+	−	−	+	−	+	+	−	−	+	+	−	−	+	+	−	−	+	+	−
+	−	−	+	+	−	−	+	−	+	+	−	−	+	+	−	+	−	−	+	+	−	−	+	−	+	+	−	−	+	+	−
+	−	−	+	+	−	−	+	−	+	+	−	−	+	+	−	−	+	+	−	−	+	+	−	+	−	−	+	+	−	−	+
+	−	+	−	−	+	−	+	+	−	+	−	−	+	−	+	+	−	+	−	−	+	−	+	+	−	+	−	−	+	−	+
+	−	+	−	−	+	−	+	+	−	+	−	−	+	−	+	−	+	−	+	+	−	+	−	−	+	−	+	+	−	+	−
+	−	+	−	−	+	−	+	−	+	−	+	+	−	+	−	+	−	+	−	−	+	−	+	−	+	−	+	+	−	+	−
+	−	+	−	−	+	−	+	−	+	−	+	+	−	+	−	−	+	−	+	+	−	+	−	+	−	+	−	−	+	−	+

TABLE V. Lattice sums over a sphere of radius 380 Å for the lattice of Gd^{3+} ions in Gd247. The variables *r, x, y, z* are the displacements and their components from an origin situated at a given ion in sublattice 1 to each ion in one of the various sublattices (see, e.g., numberings and orientations of the *x, y, z* axes in Fig. 1). The unit of length is 2 Å. All the required lattice sums can be calculated from the sums given here. (The *z* axis is parallel to the *c* axis, and the *x, y* axes are coincident with the *a, b* vectors of the unit cell, respectively. It is noted that $\Sigma(xy/r^5)=\Sigma(yz/r^5)=\Sigma(zx/r^5)=0$. The values of the unit-cell parameters used are $a=3.872$ Å, $b=3.879$ Å, $c=50.360$ Å (Ref. 3).

Sublattice summed	$\sum \frac{3z^2-r^2}{r^5}$	$\sum \frac{x^2-y^2}{r^5}$
1	−0.144 105	0.000 181
2	−0.390 903	0.255 805
3	−0.389 521	−0.255 805
4	−0.272 673	−0.000 298
5, 6	0.011 051	0.000 000
7	0.011 050	0.000 000
8	0.011 152	0.000 000
9	0.011 190	0.000 001
10	0.011 087	0.000 033
11	0.011 085	−0.000 034
12	0.010 990	0.000 000
13, 15	0.011 066	0.000 000
14, 16	0.011 065	0.000 000
17, 18, 19, 20, 21, 22, 23, 24	0.000 000	0.000 000
25, 26, 27, 28	0.011 065	0.000 000
29, 31	0.011 138	0.000 017
30, 32	0.011 038	0.000 017

described in Refs. 13 and 15, respectively, for the case of the presence of one and two R^{3+} ions in the unit cell. For *R*247 compounds, there are present four R^{3+} ions in the unit cell, involving 32 sublattices, which is also amenable to the LT method using permutation groups as discussed by Misra[12] in his generalization of the original LT method[11] to the presence of more than one ion per unit cell. The four ions in *R*247 compounds are situated at the positions (0,0,0), $(0,0,\frac{1}{4})$, $(0,\frac{1}{2},\frac{1}{2})$, and $(0,\frac{1}{2},\frac{3}{4})$ in the unit cell, and will hereafter be considered to generate sublattices 1, 2, 3, 4, respectively. Specifically, for application of the generalized LT method to *R*247 compounds, the entire lattice is subdivided into 32 sublattices, all the magnetic moments at any sublattice being oriented in the same direction. These sublattices are generated from the positions of the four R^{3+} ions in the unit cell, by the application of the translation vectors $\mathbf{\Gamma}=2l\mathbf{a}+2m\mathbf{b}+2n\mathbf{c}$, where *l, m, n* are zero, positive, or negative integers, and **a**, **b**, **c** are unit-cell vectors. Accordingly, within the framework of the LT method, the possible ordered configurations of the magnetic moments of the R^{3+} ions corresponding to the lowest energy can only be either ferromagnetic, antiferromagnetic, or layered antiferromagnetic, which are described as follows. The ferromagnetic configurations are those in which all the rare-earth magnetic moments point in the same direction, while the antiferromagnetic configurations are those in which all the adjacent magnetic moments to a rare-earth moment point in opposite directions. In layered-antiferromagnetic configurations, the adjacent moments in one plane to a rare-earth moment point in the opposite direction, while in the two perpendicular planes to this plane they point in the same direction, explicitly, for *R*123, *R*124, or *R*247 compounds they point in the opposite direction in the *ab* plane in which the nearest-neighbor distances are the shortest, and in the parallel direction in the *ac* and *bc* planes.

TABLE VI. Measured or calculated R^{3+} *g* values for *R*123 and *R*124 compounds as taken from those listed in Ref. 15. The subscripts *a, b, c* denote the *g* values along the *a, b,* and *c* axes, respectively. K and NK stand for Kramers and non-Kramers ions, respectively. EX, TH (Ref. 16), and TH-INS indicate experimentally measured, theoretically calculated values in Ref. 16, and those calculated using neutron inelastic-scattering data as mentioned in Ref. 16, respectively. The measured values are for the *R*123 compounds, while the calculated values are both for *R*123 (outside brackets) and *R*124 (within brackets). It is noted that for non-Kramers ions the *g* values of the lowest two levels are temperature dependent (Ref. 16). The values indicated here are those calculated at 5 K (for more details, see Ref. 16). g_β represents the smaller of the g_a and g_b values.

R	Ion type	g_a	g_b	g_c	g_c/g_β	Remarks
Nd	K	1.108	0.778	2.863	3.68	TH-INS
		0	0	3.636	∞	TH-INS
Yb	K	3.5	3.7	3.1	0.89	EX (EPR)
Er	K	7.1	8.4	4.1	0.58	EX (EPR)
Dy	K	2.771	1.408	13.914	9.88	TH-INS
		0.09	0.062	11.532	186	TH-INS
Ce	K	1.23 (1.29)	1.21 (1.21)	3.50 (3.45)	2.89 (2.85)	TH (Ref. 16)
		1.05 (1.31)	1.43 (1.32)	3.36 (2.35)	3.11 (1.79)	TH (Ref. 16)
Sm	K	0.89 (0.81)	0.81 (0.90)	0.29 (0.29)	0.34 (0.46)	TH (Ref. 16)
Pr	NK	0	0	4.17 (4.36)	∞	TH (Ref. 16)
Tb	NK	0	0	17.98 (17.99)	∞	TH (Ref. 16)
Ho	NK	0	0	10.86 (11.16)	∞	TH (Ref. 16)
Tm	NK	0	0	0.022 (0.87)	∞	TH (Ref. 16)

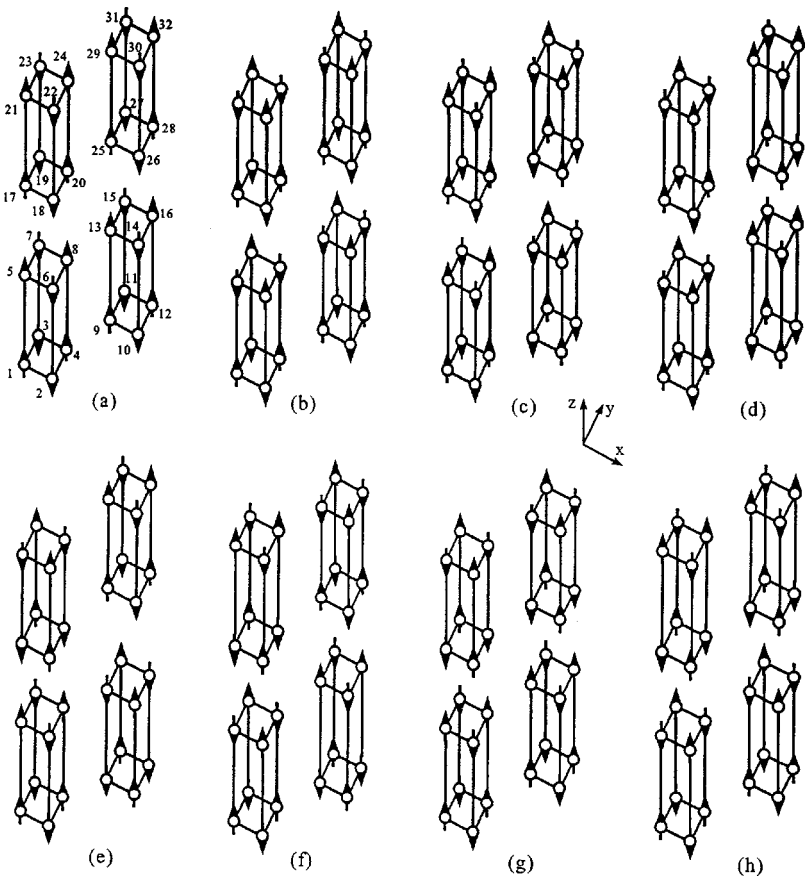

FIG. 1. The orientations of the magnetic moments of the rare-earth ions corresponding to the lowest energy, when they are oriented in the z direction, as given by Eqs. (5a) and (5b). The letters below each configuration correspond to the eigenvectors listed in Table III as follows: (a) $=q(25)$; (b)$=q(5)$; (c)$=q(27)$; (d)$=q(7)$; (e)$=q(28)$; (f)$=q(8)$; (g)$=q(26)$; (h)$=q(6)$. The numberings of the various ions correspond to the same as those used in Table V for calculating lattice sums.

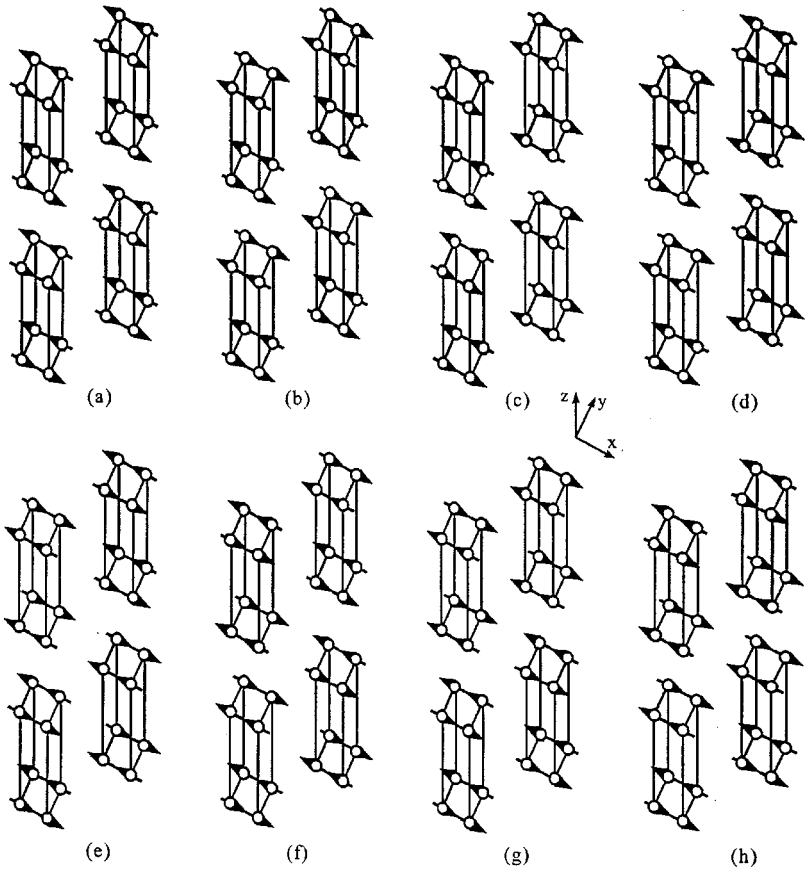

FIG. 2. The orientations of the magnetic moments of the rare-earth ions corresponding to the lowest energy, when they are oriented in the x direction, as given by Eq. (5c). The letters below each configuration correspond to the eigenvectors listed in Table III as follows: (a)$=q(9)$; (b) $=q(21)$; (c)$=q(11)$; (d)$=q(23)$; (e)$=q(12)$; (f)$=q(24)$; (g)$=q(10)$; (h)$=q(22)$. The numberings of the various ions correspond to the same as those used in Table V for calculating lattice sums, and as indicated in Fig. 1.

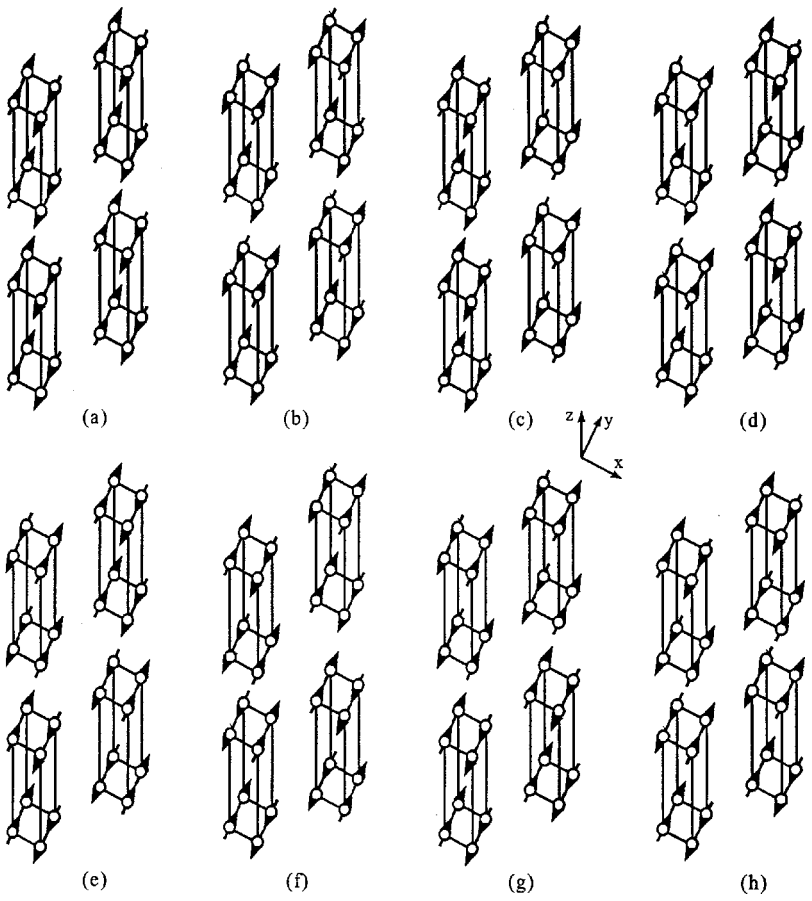

FIG. 3. The orientations of the magnetic moments of the rare-earth ions corresponding to the lowest energy, when they are oriented in the y direction, as given by Eq. (5d). The letters below each configuration correspond to the eigenvectors listed in Table III as follows: (a)$=q(17)$; (b) $=q(29)$; (c)$=q(19)$; (d)$=q(31)$; (e)$=q(20)$; (f)$=q(32)$; (g)$=q(18)$; (h)$=q(30)$. The numberings of the various ions correspond to the same as those used in Table V for calculating lattice sums, and as indicated in Fig. 1.

Results required for 32 sublattices

The permutation groups of 32 objects, P_k; $k=1,2,...,32$, as derived here are listed in Table II, while the corresponding eigenvectors, $\mathbf{q}(k)$; $k=1,2,...,32$, are listed in Table III. The eigenvalues, ε_{kj}, of P_k with respect to the eigenvector $q(j)$ are listed in Table IV. The ordered configurations are expressed as

$$\eta(k,\alpha)=q(k)\varphi(k,\alpha);\quad k=1,2,...,32;\quad \alpha=x,y,z, \tag{1}$$

where $\varphi(k,\alpha)$ are the eigenvectors of the matrix $\tilde{L}_k$, defined as

$$L_k^{\mu\nu}=\sum_{j=1}^{32} A_{ij}^{\mu\nu}\varepsilon_{P(i,j)};\quad i,j=1,2,...,32;\ \mu,\nu=x,y,z, \tag{2}$$

where the $\varepsilon_{P(i,j)}$ for permutation groups of 32 objects are the same as ε_{kj} listed in Table I. The elements $A_{ij}^{\mu\nu}$ in Eq. (2), include the dipolar and exchange interactions between an ion situated on sublattice i and all ions on sublattice j: $A_{ij}^{\mu\nu}=\{\Sigma_{\ell\varepsilon\{j\}}J_{i\ell}^{\mu\nu}\}$ for $i\neq j$; and $A_{ij}^{\mu\nu}=\{\Sigma_{\ell\varepsilon\{j\},\ell\neq i}J_{i\ell}^{\mu\nu}\}$ for $i=j$. (Here the notation $\{j\}$ means inclusion of all ions on sublattice j in the summation.) Explicitly,

$$J_{ij}^{\mu\nu}=\frac{S(S+1)}{2}\mu_B^2\left(g_{\mu\mu}g_{\nu\nu}\frac{r_{ij}^2\delta_{\mu\nu}-3r_{ij}^{\mu}r_{ij}^{\nu}}{r_{ij}^5}+v_{ij}\Delta_{ij}\delta_{ij}\right), \tag{3}$$

where the first and second terms inside the curly brackets represent dipolar and exchange interactions, respectively; S and $g_{\mu\mu}$, $g_{\nu\nu}$ $(\mu,\nu=x,y,z)$ are the effective spin and the diagonal elements of the g matrix of the rare-earth ion, respectively; μ_B is the Bohr magneton, $\mathbf{r}_{ij}$ is the vector that joins the ionic positions i and j, with the superscript μ representing its μth component; v_{ij} is the isotropic exchange interaction between the ions i and j; $\Delta_{ij}=\pm 1$ if the i, j are the nearest or next-nearest ions$=0$ otherwise, thus neglecting the exchange interactions between ions which are neither nearest nor next-nearest neighbors. The required lattice sums for dipolar interactions were evaluated with the origin being situated at the site of a rare-earth ion with respect to the various ions located on the 32 sublattices for Gd247 over a sphere of radius 380 Å, listed in Table V. Since the lattice sums are performed over a sphere it is necessary to correct for the demagnetization factor for ferromagnetic configurations, since the sample orders in long, thin needles (cylinders) to minimize its energy, which is lower than that for a spherical sample. This correction[12] is expressed as: $E_{dm}(\alpha)=-(4\pi/3)[S(S+1)/3]n_0g_{\alpha\alpha}^2$; with $n_0=(\frac{1}{32})abc$, for the magnetic moments being ordered in the α $(=x,y,z)$ direction. (Here n_0 represents the number of dipole moments per unit volume per sublattice, there being 32 sublattices for $R247$; the g matrix is diagonal in the coordinate system used here.) The required experimental g values of these have not been reported as yet. However, one can be guided by the values calculated for the $R123$ and $R124$ compounds, which

TABLE VII. Lowest lying energies and the corresponding eigenvectors, $q(k,\alpha)$ showing the orientations of the magnetic moments. Here the $q(k,\alpha)$, $\alpha(=x,y,z)$ are those depicted in Figs. 1–3. The $g_\parallel$ and $g_\perp$ values used for calculation are taken from Table VI, and represent the averages of g_a, g_b values for $g_\perp$, and one of the g_c values for $g_\parallel$ if more than one set of values are listed for an ion. K and NK stand for Kramers and non-Kramers ions, respectively. If the two lowest lying energies are extremely close to each other, then both are listed.

R	Ion type	$g_\perp$	$g_\parallel$	Lowest LT energy (K)	Orientation of moments $q(k,\alpha)$ for lowest LT energy (figure)
Nd	K	0.95	2.9	−0.0893	$q(n,z)$; $n=5-8$, 25–28 (Fig. 1)
Yb	K	3.6	3.1	−0.2658	$q(n,x)$; $n=9-12$, 21–24 (Fig. 2)
				−0.2647	$q(n,y)$; $n=17-20$, 29–32 (Fig. 3)
Er	K	7.8	4.1	−1.2478	$q(n,x)$; $n=9-12$, 21–24 (Fig. 2)
				−1.2428	$q(n,y)$; $n=17-20$, 29–32 (Fig. 3)
Dy	K	2.1	13.9	−2.0522	$q(n,z)$; $n=5-8$, 25–28 (Fig. 1)
Ce	K	1.2	3.5	−0.1301	$q(n,z)$; $n=5-8$, 25–28 (Fig. 1)
Sm	K	0.84	0.29	−0.0145	$q(n,x)$; $n=9-12$, 21–24 (Fig. 2)
				−0.0144	$q(n,y)$; $n=17-20$, 29–32 (Fig. 3)
Pr	NK	0.0	4.14	−0.1785	$q(n,z)$; $n=5-8$ (Fig. 1)
				−0.1786	$q(n,z)$; $n=25-28$ (Fig. 1)
Tb	NK	0.0	17.98	−3.4414	$q(n,z)$; $n=5-8$, 25–28 (Fig. 1)
Ho	NK	0.0	10.86	−1.2852	$q(n,z)$; $n=5-8$, 25–28 (Fig. 1)
Tm	NK	0.0	0.022/0.67	$-5.27\times10^{-6}/-4.89\times10^{-3}$	$q(n,z)$; $n=5-8$, 25–28 (Fig. 1)

have the same structure as those of the $R247$ compounds. These calculated g values and some measured ones, as given in Ref. 16, are listed in Table VI.

Finally, the energies of the ordered configurations, $E(k,\alpha)$, and the corresponding eigenvectors describing the ordering of rare-earth moments are obtained by solving the eigenvalue equation

$$\tilde{L}_k\varphi(k,\alpha)=E(k,\alpha)\varphi(k,\alpha). \tag{4}$$

It is noted from Eq. (2), and the fact that the lattice sums required in $A_{ij}^{\mu\nu}$ are zero for $\mu\neq\nu$, as seen from Table V, that the eigenvectors $\varphi(k,\alpha)$ are such that the magnetic moments on anyone of the 32 sublattices are all oriented along the α $(=x,y,z)$ directions corresponding to the eigenvectors $\eta(k)$, as given by Eq. (1), and listed in Table III, with the elements $+1$ and -1 indicating the direction to be parallel to α and $-\alpha$ directions, respectively.

III. CALCULATED LOWEST ENERGY CONFIGURATIONS FOR $R247$ COMPOUNDS

General results

In general, as for the lowest lying dipolar energies (eigenvalues) calculated for the various $R247$ compounds using the LT method, the following is noted. The two lowest lying energies (in units of K) for the orientations of the magnetic moments parallel and perpendicular to the z axis, and the corresponding configurations $\eta(k,\alpha)$; $\alpha=x,y,z$; $k=1-32$, of the various $R247$ compounds, as calculated using the generalized LT method for 32 sublattices, taking into account both the dipolar and exchange interactions, are

$$E(k,z)(k=5,6,25,26) = -0.010\,6216g_{zz}^2-2v_{n'}-2v_{n''}+4v_{n'''} \tag{5a}$$

$$E(k,z)(k=7,8,27,28) = -0.010\,6211g_{zz}^2-2v_{n'}-2v_{n''}+4v_{n'''} \tag{5b}$$

$$E(k,x)(k=9,10,11,12,21,22,23,24) = -0.0205097g_{xx}^2+2v_{n'}-2v_{n''}-4v_{n'''} \tag{5c}$$

$$E(k,y)(k=17,18,19,20,29,30,31,32) = -0.0204274g_{yy}^2-2v_{n'}+2v_{n''}-4v_{n'''}. \tag{5d}$$

In Eqs. (5a)–(5d), the $v_{n'}$, $v_{n''}$, $v_{n'''}$ terms represent the contributions of the exchange interaction, assumed to be isotropic, with the nearest, next-nearest, and next-next-nearest neighbors, respectively, while the terms in g_{xx}, g_{yy}, g_{zz} represent the contribution of the dipolar interaction. To an ion on sublattice 1, the two nearest neighbors are situated on sublattice 2, the two next-nearest neighbors on sublattice 3, and the four next-next-nearest neighbors on sublattice 4 at distances 3.872, 3.879, and 5.481 Å, respectively. It is further noted that for all configurations k, given in each of Eqs. (5a)–(5d), the lowest energy possesses the same dipolar and exchange energies. These configurations of lowest energy, which are all layered antiferromagnetic, as indicated by Eqs. (5a)–(5d), are shown in Figs. 1, 2, and 3, respectively, wherein the rare-earth moments point in the z, x, and y directions, respectively.

An analysis of the energies given by Eqs. (5a)–(5d) reveals the following. For the same values of g_{xx} and g_{yy}, the lowest dipolar energy corresponding to the eight y configurations, as given by Eq. (5d), is very slightly higher than that of the eight x configurations, as given by Eq. (5c), due to the slight orthorhombic distortion from the tetragonal symmetry of the $R247$ lattice. Finally, the ordering with the lowest energy will correspond to $q(kz)$, $k=5-8$, 25–28 if g_{zz}

$>1.3895\, g_{\beta\beta}$, while it will be $q(kx)$, $k=9-12$, 21–24, or $q(ky)$, $k=17-20$, 29–32 if $g_{zz}<1.3895\, g_{\beta\beta}$, where $g_{\beta\beta}$ represents the smaller of g_{xx} and g_{yy}, ignoring the small difference between the x/y orderings as given by Eqs. (4c) and (4d). The exchange interactions have the same contribution for each of the energy given by Eqs. (4a)–(4d). They can, however, be important for the case $g_{zz}\sim 1.3895 g_{\beta\beta}$ ($\beta=x,y$). When $g_{xx}^2>0.996 g_{yy}^2$ for the case $g_{zz}<1.3895 g_{\beta\beta}$, the antiferromagnetic configurations $q(nx)$, $n=9-12$, 21–24 with the moments pointing in the x direction will be favored as these configurations then have lower energies than those of the configurations $\eta(k,y)$, $k=17-20$, 29–32 with the moments pointing in the y direction. If this is not the case, then for $g_{xx}^2>0.996 g_{yy}^2$ the antiferromagnetic configurations $\eta(k,y)$, $k=17-20$, 29–32 with the moments pointing in the y direction will be energetically favored. The relative order of the energies of these antiferromagnetic configurations may be significantly modified from those dictated by the dipolar interaction alone if the exchange interactions are sufficiently large. The exact relative order will be determined by the values of the exchange interactions as exhibited by Eqs. (4a)–(4d). In addition, if the exchange interaction is anisotropic, the relative order of the energies would also be affected.

IV. PARTICULAR RESULTS

A. Dy247 and Er247 compounds

These compounds are the only ones whose low-temperature orderings have been determined experimentally by neutron scattering.[5,6] If one assumes the same g values as those listed in Table VI, and the same values of the exchange interactions for Er^{3+} and Dy^{3+} ions as reported by Böttger *et al.*[7–9] (see Sec. I), whose contributions are an order of magnitude smaller than those of the dipolar interactions, then the ratios $g_{zz}/g_{\beta\beta}$ ($\beta=x,y$) dictate that Dy^{3+} ions would order antiferromagnetically (layered) with the moments in the z direction given by Eqs. (5a) and (5b), while Er^{3+} ions would order antiferromagnetically (layered) with the moments in the y direction given by Eq. (5d).[6] This is in agreement with the experimental results on Er247 (Ref. 6) and Dy247, for which $q(19,y)$ and $q(25,z)$, respectively, have been reported to correspond to the low-temperature ordering. The values of the lowest energies and the corresponding orderings of magnetic moments for Dy247 and Er247 compounds are listed in Table VII.

B. Other *R*247 compounds

Using the same g values as those listed in Table VI, the values of the lowest energies and corresponding orientations of the magnetic moments are listed in Table VII, as calculated using the LT method which enables calculation of the lowest energy and the corresponding configuration. The following configurations are found to be consistent with the lowest dipolar energy, based on the ratios $g_{zz}/g_{\beta\beta}$ ($\beta=x,y$): $\eta(k,z)$, $k=5-8$, 25–28 for $R=$Nd, Dy, Ce, Pr, Gd, Tb, Ho, and Tm and $\eta(k,x)$, $k=9-12$, 21–24, or $\eta(k,y)$; $k=17-20$, 29–32 for $R=$Yb, Er, and Sm. These are found to be similar to those predicted for $R123$ (Refs. 13 and 14) and $R124$ (Ref. 15) compounds on the basis of the LT method.

ACKNOWLEDGMENT

S.K.M. acknowledges partial financial support from the Natural Sciences and Engineering Research Council of Canada.

[1] T. Kogure, R. Kontra, G. J. Yurek, and J. B. Vander Sande, Physica C **156**, 45 (1988).
[2] P. Bordet, C. Chaillout, J. Chenavas, J. L. Hodeau, M. Marezio, J. Karpinski, and E. Kaldis, Nature (London) **334**, 596 (1988).
[3] D. E. Morris, G. Asmar, J. Y. T. Wei, J. H. Nickel, R. L. Sid, J. S. Scott, and J. E. Post, Phys. Rev. B **40**, 11 406 (1989).
[4] J. L. Tallon, D. M. Pooke, R. G. Buckley, M. R. Presland, and F. J. Blunt, Phys. Rev. B **41**, 7220 (1990).
[5] H. Zhang, J. W. Lynn, and D. E. Morris, Phys. Rev. B **45**, 10 022 (1992).
[6] G. Böttger, P. Fischer, A. Dönni, P. Berastegui, Y. Aoki, H. Sato, and F. Fauth, Phys. Rev. B **55**, R12 005 (1997).
[7] G. Böttger, P. Allenspach, A. Dönni, Y. Aoki, and H. Sato, Z. Phys. B: Condens. Matter **104**, 195 (1997).
[8] G. Böttger, P. Fischer, A. Dönni, Y. Aoki, H. Sato, and P. Berastegui, J. Magn. Magn. Mater. **177–181**, 517 (1998).
[9] G. Böttger, P. Allenspach, J. Mesot, A. Dönni, Y. Aoki, and H. Sato, J. Alloys Compd. **275–277**, 560 (1998).
[10] H. Zhang, J. W. Lynn, and D. E. Morris, J. Magn. Magn. Mater. **104–107**, 821 (1992).
[11] J. M. Luttinger and L. Tisza, Phys. Rev. **70**, 954 (1946).
[12] S. K. Misra, Phys. Rev. B **8**, 2026 (1973).
[13] S. K. Misra and J. Felsteiner, Phys. Rev. B **46**, 11 033 (1992).
[14] A. G. Anders and S. V. Volotskii, Sverkhprovodimost' (KIAE) **5**, 575 (1992) [Superconductivity **5**, 575 (1992)].
[15] J. Felsteiner and S. K. Misra, Phys. Rev. B **50**, 7184 (1994).
[16] S. K. Misra, Y. Chang, and J. Felsteiner, J. Phys. Chem. Solids **58**, 1 (1997).